

# Magnetic phase diagram of the half-filled $t - t'$ -Hubbard model — finite- $U$ effects on competing interactions and frustration

Avinash Singh

*Department of Physics, Indian Institute of Technology, Kanpur - 208016, India*

The magnon propagator is evaluated in the AF  $(\pi, \pi, \pi)$  and the F-AF  $(0, \pi, \pi)$  states at the RPA level, and the spin-fluctuation corrections are compared. Transverse spin fluctuations are sharply enhanced by the frustration-inducing NNN hopping  $t'$ , reducing the zero-temperature AF order in two dimensions, and the Néel temperature in three dimensions. The phase boundary between the insulating AF and F-AF states is obtained in the full range of interaction strength, indicating that the AF state is interestingly stabilized with decreasing  $U$ .

75.10.Jm, 75.10.Lp, 75.30.Ds, 75.10.Hk

## I. INTRODUCTION

The magnetic properties of correlated electron systems have been of immense interest in recent years. In terms of the Hubbard model representation involving a correlation term  $U$  and a nearest-neighbour (NN) hopping term  $t$ , the antiferromagnetic (AF) insulating state at half filling has been studied in considerable detail. Various properties characterizing spin fluctuations, such as the magnon velocity, [1,2] sublattice magnetization, [1,3] Néel temperature, [4] and the integrated spectral weight of transverse spin fluctuations, [5] have been obtained in the full  $U$  range. All results properly interpolate between the weak-coupling SDW limit and the strong-coupling QHAF limit. Thus, the approach of incorporating quantum spin-fluctuation corrections about the HF-level broken-symmetry state, either within a systematic, perturbation-theoretic, inverse-degeneracy expansion, [6] or at the self-consistently renormalized level, [4] has been successfully carried over to the strong coupling limit.

In the strong coupling limit, the next-nearest-neighbour (NNN) hopping term  $t'$  introduces a NNN AF spin coupling  $J' = 4t'^2/U$  in the equivalent  $S = 1/2$  quantum Heisenberg antiferromagnetic (QHAF) model which, in the AF ground state, competes with the NN AF coupling  $J = 4t^2/U$ . The consequent frustration effects have been studied earlier for the QHAF on a square lattice. [7,8] In the classical limit ( $S \rightarrow \infty$ ), the AF state is unstable for  $J' > J/2$  towards a state having AF ordering in each sublattice, with arbitrary angle  $\theta$  between the sublattice magnetization directions. Linear spin-wave analysis yields negative energy modes except when  $\theta = 0, \pi$ . [8] Hence the point  $J'/J = 1/2$  marks the boundary between the AF phase with ordering wavevector  $\mathbf{Q} = (\pi, \pi)$  and a F-AF phase with  $\mathbf{Q} = (\pi, 0)$  or  $(0, \pi)$ , involving ferromagnetic and antiferromagnetic orderings in the two directions.

For large but finite  $U$ , the expansion in powers of  $t/U$  leads to higher-order spin couplings besides the NN AF coupling  $J$ . The next terms are NNN and NNNN *ferromagnetic* couplings of order  $t^4/U^3$ , which connect sites of the same sublattice; their effect on the magnon spec-

trum has been discussed earlier within a systematic expansion for the transverse spin propagator. [9] The competition between the NNN ferromagnetic coupling of order  $Jt^2/U^2$  and the NNN AF coupling of order  $Jt'^2/t^2$  implies a reduction in the frustration, suggesting a finite- $U$  stabilization of the AF state. With decreasing  $U$ , even more extended-range spin couplings become important, and a weak-coupling approach becomes more meaningful.

In this paper we study this magnetic competition and frustration in the full  $U$  range, and obtain the RPA-level magnetic phase diagram of the half-filled  $t - t'$ -Hubbard model in  $d = 3$ . The AF state, as expected, is stabilized at finite  $U$ , and the AF—F-AF phase boundary is pushed to higher  $t'$  values. We have also quantitatively studied, in the strong coupling limit, the effects of the  $J'$ -induced frustration on the transverse spin fluctuations, resulting in enhancement of the quantum correction to sublattice magnetization in two dimensions, and suppression of Néel temperature in three dimensions. Furthermore, we have extended the evaluation of the magnon propagator to the more complicated F-AF ground states with ordering wavevectors  $(0, \pi)$  and  $(0, \pi, \pi)$ .

The need for more realistic microscopic models which include NNN hopping etc., has been acknowledged recently from band structure studies, photoemission data and neutron-scattering measurements of high- $T_c$  and related materials. [10–13] Estimates for  $|t'/t|$  range from 0.15 to 0.5. Effect of hole and electron doping on the commensurate spin ordering have been studied for the  $t - t'$ -Hubbard model and applied to  $\text{La}_{2-x}\text{Sr}_x\text{CuO}_4$  and  $\text{Nd}_{2-x}\text{Ce}_x\text{CuO}_4$ . [14] Spin correlation function, incommensurability, and local magnetic moments in the doped  $t - t'$ -Hubbard model have been studied using the Quantum Monte Carlo method. [15] At half filling, existence of an antiferromagnetic metallic (AFM) phase has been suggested in  $d = 2$  [16] and  $d = 3$ . [17] The suppression of the perfect-nesting instability by the NNN hopping, and the critical interaction  $U_c$  vs.  $t'$  phase diagram has been studied in  $d = 2, 3$ . [17] Magnon softening due to  $t'$  and a significant enhancement in the low-energy spectral function due to single-particle excitations has also been observed. [5]

## II. HUBBARD MODEL WITH NEXT-NEAREST-NEIGHBOUR HOPPING

We consider the  $t - t'$ -Hubbard model, with hopping terms  $t$  and  $t'$  between nearest-neighbour (NN) pairs of sites  $i$  and  $i + \delta$ , and next-nearest-neighbour (NNN) pairs of sites  $i$  and  $i + \kappa$ , respectively:

$$H = -t \sum_{i,\delta,\sigma} a_{i,\sigma}^\dagger a_{i+\delta,\sigma} - t' \sum_{i,\kappa,\sigma} a_{i,\sigma}^\dagger a_{i+\kappa,\sigma} + U \sum_i n_{i\uparrow} n_{i\downarrow}. \quad (1)$$

For concreteness, we have considered the square lattice and the simple cubic lattice. In the plane-wave basis defined by  $a_{i\sigma} = \sqrt{\frac{1}{N}} \sum_{\mathbf{k}} e^{i\mathbf{k}\cdot\mathbf{r}_i} a_{\mathbf{k}\sigma}$ , the free-fermion part of the Hamiltonian  $H_0 = \sum_{\mathbf{k}\sigma} (\epsilon_{\mathbf{k}} + \epsilon'_{\mathbf{k}}) a_{\mathbf{k}\sigma}^\dagger a_{\mathbf{k}\sigma}$ , where

$$\begin{aligned} \epsilon_{\mathbf{k}} &= -t \sum_{\delta} e^{i\mathbf{k}\cdot\delta} \\ \text{and } \epsilon'_{\mathbf{k}} &= -t' \sum_{\kappa} e^{i\mathbf{k}\cdot\kappa} \end{aligned} \quad (2)$$

are the two free-fermion energies, corresponding to NN and NNN hopping, respectively.

For the NN hopping model, the HF-level description of the broken-symmetry AF state, and transverse spin fluctuations about this state have been studied earlier in the strong, intermediate, and weak coupling limits. [2,9,18] Since the NNN hopping term  $t'$  connects sites in the same sublattice, the corresponding  $\epsilon'_{\mathbf{k}}$  term appears, in the two-sublattice basis, in the diagonal matrix elements of the HF Hamiltonian;

$$H_{\text{HF}}^\sigma(\mathbf{k}) = \begin{bmatrix} -\sigma\Delta + \epsilon'_{\mathbf{k}} & \epsilon_{\mathbf{k}} \\ \epsilon_{\mathbf{k}} & \sigma\Delta + \epsilon'_{\mathbf{k}} \end{bmatrix} = \epsilon'_{\mathbf{k}} \mathbf{1} + \begin{bmatrix} -\sigma\Delta & \epsilon_{\mathbf{k}} \\ \epsilon_{\mathbf{k}} & \sigma\Delta \end{bmatrix} \quad (3)$$

for spin  $\sigma$ . Here  $2\Delta = mU$ , where  $m$  is the sublattice magnetization, and for the NN hopping model  $2\Delta$  is also the energy gap for single-particle excitations. Since the  $\epsilon'_{\mathbf{k}}$  term appears as a unit matrix, the eigenvectors of the HF Hamiltonian remain unchanged from the NN case, whereas the eigenvalues corresponding to the quasiparticle energies are modified to

$$E_{\mathbf{k}\sigma}^{(\pm)} = \epsilon'_{\mathbf{k}} \pm \sqrt{\Delta^2 + \epsilon_{\mathbf{k}}^2}, \quad (4)$$

the two signs  $\pm$  referring to the two quasiparticle bands. The band gap is thus affected by the NNN hopping term, and in the strong coupling limit ( $2\Delta \approx U$ ) it approximately decreases as  $U - 4t'$  for  $J \gg t'$  and as  $U - 8t'$  for  $J \ll t'$  in  $d = 2$ .

The fermionic quasiparticle amplitudes  $a_{\mathbf{k}\sigma}$  and  $b_{\mathbf{k}\sigma}$  on the two sublattices A and B, for spin  $\sigma = \uparrow, \downarrow$  and the two quasiparticle bands  $\ominus, \oplus$ , are given by

$$\begin{aligned} a_{\mathbf{k}\uparrow\ominus}^2 &= b_{\mathbf{k}\downarrow\ominus}^2 = a_{\mathbf{k}\downarrow\oplus}^2 = b_{\mathbf{k}\uparrow\oplus}^2 = \frac{1}{2} \left( 1 + \frac{\Delta}{\sqrt{\Delta^2 + \epsilon_{\mathbf{k}}^2}} \right) \\ a_{\mathbf{k}\uparrow\oplus}^2 &= b_{\mathbf{k}\downarrow\oplus}^2 = a_{\mathbf{k}\downarrow\ominus}^2 = b_{\mathbf{k}\uparrow\ominus}^2 = \frac{1}{2} \left( 1 - \frac{\Delta}{\sqrt{\Delta^2 + \epsilon_{\mathbf{k}}^2}} \right). \end{aligned} \quad (5)$$

These relationships follow from the spin-sublattice and particle-hole symmetry in the AF state. The above two expressions provide the majority and minority fermionic densities. On the A-sublattice, the majority density is of spin  $\uparrow$  ( $\downarrow$ ) states in the lower (upper) band.

As the eigenvectors of  $H_{\text{HF}}^\sigma(\mathbf{k})$  are unchanged, the self-consistency condition retains its form provided the band gap is finite, and therefore the sublattice magnetization is independent of  $t'$ . We will restrict ourselves to this insulating regime with no band overlap. When the bands begin to overlap, and some upper band states get occupied, the spin- $\downarrow$  density (on the A-sublattice) increases at the expense of spin- $\uparrow$  density. The consequent reduction in the sublattice magnetization  $m$  (and therefore  $\Delta$ ) further increases the band overlap, which results in a drastic reduction of  $m$ . For  $d = 2$  it was found [17] that for  $t'$  below a threshold value  $t'_0 \approx 0.4$  the AF order jumps to 0 discontinuously when  $U$  is reduced below a critical value  $U_c(t')$ , indicating a first-order phase transition. However, for  $t' > t'_0$ , the AF order decreases to zero continuously, but extremely fast. In  $d = 3$  the antiferromagnetic metallic (AFM) state survives in a relatively broader  $U$  range.

## III. THE MAGNON PROPAGATOR

The magnon (transverse spin fluctuation) propagator in the AF state, with ordering in the  $z$  direction, is obtained from the time-ordered propagator of the transverse spin operators  $S_i^-$  and  $S_j^+$  at sites  $i$  and  $j$ ;

$$\begin{aligned} \chi^{-+}(\mathbf{q}, \omega) &= \int dt \sum_i e^{i\omega(t-t')} e^{-i\mathbf{q}\cdot(\mathbf{r}_i - \mathbf{r}_j)} \times \\ \langle \Psi_{\text{G}} | T [S_i^-(t) S_j^+(t')] | \Psi_{\text{G}} \rangle &= \frac{[\chi^0(\mathbf{q}, \omega)]}{[1 - U\chi^0(\mathbf{q}, \omega)]} \end{aligned} \quad (6)$$

at the RPA (ladder-sum) level. Here the zeroth-order particle-hole propagator,  $[\chi^0(\mathbf{q}, \omega)] = i \int \frac{d\omega'}{2\pi} \sum_{\mathbf{k}} [G^\uparrow(\mathbf{k}'\omega')] [G^\downarrow(\mathbf{k}' - \mathbf{q}, \omega' - \omega)]$ , is evaluated in the broken-symmetry AF state. Evaluation of the magnon-mode energies is facilitated by expressing the  $2 \times 2$  matrix  $[\chi^0(\mathbf{q}, \omega)]$  in terms of its eigenvalues  $\lambda_{\mathbf{q}}^n(\omega)$  and eigenvectors  $|\phi_{\mathbf{q}}^n(\omega)\rangle$ ;

$$[\chi^{-+}(\mathbf{q}, \omega)]_{\text{RPA}} = \sum_{n=1,2} \left( \frac{\lambda_{\mathbf{q}}^n(\omega)}{1 - U\lambda_{\mathbf{q}}^n(\omega)} \right) |\phi_{\mathbf{q}}^n(\omega)\rangle \langle \phi_{\mathbf{q}}^n(\omega)|, \quad (7)$$

and the magnon energies are then obtained from the pole  $1 - U\lambda_{\mathbf{q}}^n(\omega) = 0$ .

In the AFI state, with only interband particle-hole processes, the bare propagator  $[\chi^0(\mathbf{q}, \omega)]$  is given by [2]

$$[\chi^0(\mathbf{q}, \omega)] = \sum_{\mathbf{k}} \begin{bmatrix} a_{\mathbf{k}\uparrow\oplus}^2 a_{\mathbf{k}-\mathbf{q}\downarrow\oplus}^2 & a_{\mathbf{k}\uparrow\oplus} b_{\mathbf{k}\uparrow\oplus} a_{\mathbf{k}-\mathbf{q}\downarrow\oplus} b_{\mathbf{k}-\mathbf{q}\downarrow\oplus} \\ a_{\mathbf{k}\uparrow\oplus} b_{\mathbf{k}\uparrow\oplus} a_{\mathbf{k}-\mathbf{q}\downarrow\oplus} b_{\mathbf{k}-\mathbf{q}\downarrow\oplus} & b_{\mathbf{k}\uparrow\oplus}^2 b_{\mathbf{k}-\mathbf{q}\downarrow\oplus}^2 \end{bmatrix} \frac{1}{E_{\mathbf{k}-\mathbf{q}}^{\oplus} - E_{\mathbf{k}}^{\ominus} + \omega - i\eta} + \sum_{\mathbf{k}} \begin{bmatrix} a_{\mathbf{k}\uparrow\oplus}^2 a_{\mathbf{k}-\mathbf{q}\downarrow\ominus}^2 & a_{\mathbf{k}\uparrow\oplus} b_{\mathbf{k}\uparrow\oplus} a_{\mathbf{k}-\mathbf{q}\downarrow\ominus} b_{\mathbf{k}-\mathbf{q}\downarrow\ominus} \\ a_{\mathbf{k}\uparrow\oplus} b_{\mathbf{k}\uparrow\oplus} a_{\mathbf{k}-\mathbf{q}\downarrow\ominus} b_{\mathbf{k}-\mathbf{q}\downarrow\ominus} & b_{\mathbf{k}\uparrow\oplus}^2 b_{\mathbf{k}-\mathbf{q}\downarrow\ominus}^2 \end{bmatrix} \frac{1}{E_{\mathbf{k}}^{\oplus} - E_{\mathbf{k}-\mathbf{q}}^{\ominus} - \omega - i\eta}. \quad (8)$$

in terms of the fermionic quasiparticle amplitudes and energies. In the AFM state, additional (intra-band) processes involving particle-hole excitations from the same band would also contribute. Evaluation of  $[\chi^0(\mathbf{q}, \omega)]$  and the RPA-level magnon propagator  $\chi^{-+}(\mathbf{q}, \omega)$  in the strong coupling limit is described in the next section for several lattices and broken-symmetry states. For arbitrary  $U$ , the  $\mathbf{k}$ -sum in Eq. (8) is performed numerically, and the matrix  $[\chi^0(\mathbf{q}, \omega)]$  then diagonalized to obtain the two eigenvalues  $\lambda_{\mathbf{q}}^n$  and eigenvectors  $|\phi_{\mathbf{q}}^n\rangle$ . Evaluation of the magnon velocity, and determination of the magnetic phase diagram of the  $t-t'$ -Hubbard model is described in section V.

#### IV. STRONG COUPLING LIMIT

The analytically simple strong coupling limit is considered in this section. Focussing on the enhancement of transverse spin fluctuations by the NNN hopping, we examine the magnon energy spectrum at the RPA level, and their contribution to the quantum spin-fluctuation correction  $\delta m_{\text{SF}}$  to the sublattice magnetization for a square lattice (sub-section A), and the reduction in the Néel temperature  $T_{\text{N}}$  for a simple cubic lattice (sub-section B). The RPA-level magnon propagator is also evaluated in the F-AF ground state, with ordering wavevector  $(0, \pi, \pi)$  (sub-section C).

##### A. $d = 2$

In the strong coupling limit, the majority and minority quasiparticle densities are given by  $a_{\mathbf{k}\uparrow\oplus}^2 = a_{\mathbf{k}\downarrow\oplus}^2 \approx 1 - \epsilon_{\mathbf{k}}^2/4\Delta^2$  and  $a_{\mathbf{k}\uparrow\oplus}^2 = a_{\mathbf{k}\downarrow\ominus}^2 \approx \epsilon_{\mathbf{k}}^2/4\Delta^2$ . Substituting these in Eq. (8), along with the quasiparticle energies from Eqs. (4), we obtain, for the AA matrix element

$$[\chi^{-+}(\mathbf{q}, \omega)] = -\frac{1}{2} \left( \frac{2J}{\omega_{\mathbf{q}}} \right) \begin{bmatrix} 1 - \frac{J'}{J}(1 - \gamma'_{\mathbf{q}}) - \frac{\omega}{2J} & -\gamma_{\mathbf{q}} \\ -\gamma_{\mathbf{q}} & 1 - \frac{J'}{J}(1 - \gamma'_{\mathbf{q}}) + \frac{\omega}{2J} \end{bmatrix} \left( \frac{1}{\omega - \omega_{\mathbf{q}} + i\eta} - \frac{1}{\omega + \omega_{\mathbf{q}} - i\eta} \right), \quad (12)$$

where the magnon-mode energy  $\omega_{\mathbf{q}}$  is given by

$$\left( \frac{\omega_{\mathbf{q}}}{2J} \right)^2 = \left\{ 1 - \frac{J'}{J}(1 - \gamma'_{\mathbf{q}}) \right\}^2 - \gamma_{\mathbf{q}}^2. \quad (13)$$

$$[\chi^0(\mathbf{q}, \omega)]_{\text{AA}} = \sum_{\mathbf{k}} \frac{(1 - \epsilon_{\mathbf{k}}^2/4\Delta^2)(1 - \epsilon_{\mathbf{k}-\mathbf{q}}^2/4\Delta^2)}{\sqrt{\Delta^2 + \epsilon_{\mathbf{k}}^2} + \sqrt{\Delta^2 + \epsilon_{\mathbf{k}-\mathbf{q}}^2} + (\epsilon'_{\mathbf{k}-\mathbf{q}} - \epsilon'_{\mathbf{k}}) + \omega} + \sum_{\mathbf{k}} \frac{(\epsilon_{\mathbf{k}}^2/4\Delta^2)(\epsilon_{\mathbf{k}-\mathbf{q}}^2/4\Delta^2)}{\sqrt{\Delta^2 + \epsilon_{\mathbf{k}}^2} + \sqrt{\Delta^2 + \epsilon_{\mathbf{k}-\mathbf{q}}^2} + (\epsilon'_{\mathbf{k}} - \epsilon'_{\mathbf{k}-\mathbf{q}}) - \omega}, \quad (9)$$

where  $\epsilon_{\mathbf{k}} = -2t(\cos k_x + \cos k_y)$  and  $\epsilon'_{\mathbf{k}} = -4t' \cos k_x \cos k_y$ . Expanding the denominators in powers of  $t/\Delta$ ,  $t'/\Delta$ ,  $\omega/\Delta$ , and systematically retaining terms only up to order  $t^2/\Delta^2$  and  $t'^2/\Delta^2$ , we obtain after performing the  $\mathbf{k}$ -sums, with  $\sum_{\mathbf{k}} \epsilon_{\mathbf{k}}^2 = 4t^2$ ,  $\sum_{\mathbf{k}} \epsilon'_{\mathbf{k}}^2 = 4t'^2$ , and  $\sum_{\mathbf{k}} \epsilon'_{\mathbf{k}} \epsilon'_{\mathbf{k}-\mathbf{q}} = 4t'^2 \cos q_x \cos q_y$

$$[\chi^0(\mathbf{q}, \omega)]_{\text{AA}} = \frac{1}{2\Delta} \left[ 1 - \frac{4t^2}{\Delta^2} + \frac{2t'^2}{\Delta^2}(1 - \cos q_x \cos q_y) - \frac{\omega}{2\Delta} \right] = \frac{1}{U} \left[ 1 - \frac{2t^2}{\Delta^2} \left( 1 + \frac{\omega}{2J} \right) + \frac{2t'^2}{\Delta^2}(1 - \cos q_x \cos q_y) \right], \quad (10)$$

where  $2\Delta = mU \approx (1 - 2t^2/\Delta^2)U$  and  $J = 4t^2/U$ . Similarly evaluating the other matrix elements, we obtain

$$[1 - U\chi^0(\mathbf{q}, \omega)] = \frac{2t^2}{\Delta^2} \begin{bmatrix} 1 - \frac{J'}{J}(1 - \gamma'_{\mathbf{q}}) + \frac{\omega}{2J} & \gamma_{\mathbf{q}} \\ \gamma_{\mathbf{q}} & 1 - \frac{J'}{J}(1 - \gamma'_{\mathbf{q}}) - \frac{\omega}{2J} \end{bmatrix}, \quad (11)$$

where  $\gamma_{\mathbf{q}} = (\cos q_x + \cos q_y)/2$  and  $\gamma'_{\mathbf{q}} = \cos q_x \cos q_y$ . Here  $J = 4t^2/U$  and  $J' = 4t'^2/U$  are the NN and NNN spin couplings in the equivalent Heisenberg model, and the NNN term  $J'(1 - \gamma'_{\mathbf{q}})$  directly leads to a softening of the magnon mode energies. Substituting in the RPA expression, we finally obtain for the transverse spin propagator

In the long wavelength limit ( $q \rightarrow 0$ ), with  $\gamma'_{\mathbf{q}} = \cos q_x \cos q_y \approx (1 - q_x^2/2)(1 - q_y^2/2) \approx 1 - q^2/2$ , and  $\gamma_{\mathbf{q}} = (\cos q_x + \cos q_y)/2 \approx 1 - q^2/4$ , the magnon energy reduces to

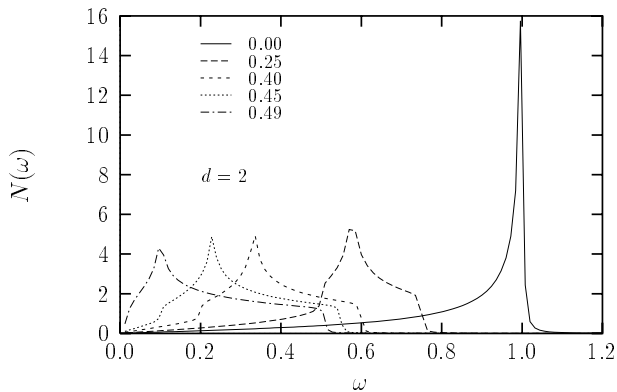


FIG. 1. The magnon density of states for different values of  $J'/J$ , showing the magnon softening and transfer of spectral weight to the low-energy region.

$$\omega_{\mathbf{q}} = \sqrt{2}Jq \left(1 - \frac{2J'}{J}\right)^{1/2}, \quad (14)$$

showing the strong softening of low-energy modes by the NNN hopping. The spin-wave velocity vanishes in the limit  $J'/J \rightarrow 1/2$ , indicating the instability of the AF state towards the F-AF state with  $\mathbf{Q} = (0, \pi)$  or  $\mathbf{Q} = (\pi, 0)$ , which is examined in the next subsection. The magnon density of states evaluated from Eq. (13) is shown in Fig. 1 for different values of  $J'/J$ . NNN hopping clearly softens the magnon modes, and transfers the magnon spectral weight to the low-energy region.

To examine the enhancement in the transverse spin fluctuations due to the strong magnon softening, we evaluate the transverse spin correlations. [3,4] From Eq. (12) for the transverse spin propagator, we obtain the local transverse spin correlations by integrating over the frequency and summing over the  $\mathbf{q}$  modes

$$\langle S^+ S^- + S^- S^+ \rangle_{\text{RPA}} = \sum_{\mathbf{q}} \frac{2J}{\omega_{\mathbf{q}}} \left\{ 1 - \frac{J'}{J} (1 - \gamma'_{\mathbf{q}}) \right\}. \quad (15)$$

The spin-fluctuation correction to sublattice magnetization is then obtained from [3,4]

$$\delta m_{\text{SF}} = \frac{\langle S^+ S^- + S^- S^+ \rangle_{\text{RPA}}}{\langle S^+ S^- - S^- S^+ \rangle_{\text{RPA}}} - 1 \quad (16)$$

where the denominator  $\langle S^+ S^- - S^- S^+ \rangle_{\text{RPA}}$  is precisely 1 for  $S = 1/2$  due to the commutation relation  $[S^+, S^-] = 2S^z$ . The spin-fluctuation correction to sublattice magnetization, evaluated from Eqs. (15), (16) is shown in

$$[\chi^{-+}(\mathbf{q}, \omega)] = -\frac{1}{2} \left( \frac{J}{\omega_{\mathbf{q}}} \right) \begin{bmatrix} \left(1 + \frac{2J'}{J}\right) - (1 - \cos q_x) - \frac{\omega}{2J} & -\cos q_y \left(1 + \frac{2J'}{J} \cos q_x\right) \\ -\cos q_y \left(1 + \frac{2J'}{J} \cos q_x\right) & \left(1 + \frac{2J'}{J}\right) - (1 - \cos q_x) + \frac{\omega}{2J} \end{bmatrix} \left( \frac{1}{\omega - \omega_{\mathbf{q}}} - \frac{1}{\omega + \omega_{\mathbf{q}}} \right), \quad (18)$$

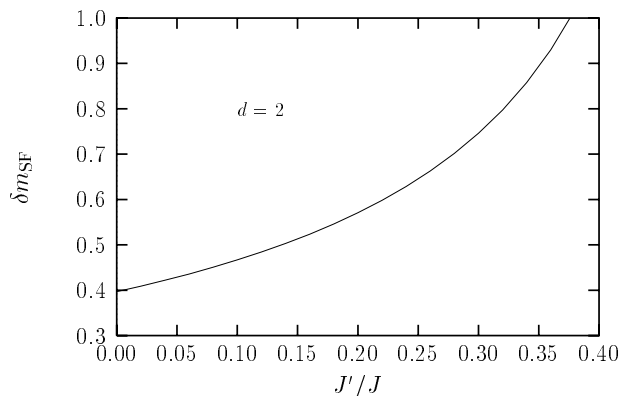


FIG. 2. The rapid increase in the spin-fluctuation correction to sublattice magnetization with the frustrating NNN spin coupling  $J'$ .

Fig. 2, showing the rapid rise in transverse spin fluctuations with the frustrating NNN spin coupling  $J'$ . The correction diverges as  $J'/J \rightarrow 1/2$ .

### B. $\mathbf{Q} = (0, \pi)$ phase

In this phase, the spin ordering along x and y directions is ferromagnetic and antiferromagnetic, respectively. The chains in the y direction may be subdivided into two sublattices, and any site  $i$  with position coordinates  $(i_x, i_y)$  may then be uniquely placed in one of the two sublattices. The NNN hopping term connects sites of opposite sublattices, while the NN hopping terms in the x and y directions connect sites of the same and opposite sublattices, respectively. Therefore, the HF Hamiltonian matrix takes the form

$$H_{\text{HF}}^{\sigma}(\mathbf{k}) = \begin{bmatrix} -\sigma\Delta + \epsilon_{\mathbf{k}}^x & \epsilon_{\mathbf{k}}^y + \epsilon'_{\mathbf{k}} \\ \epsilon_{\mathbf{k}}^y + \epsilon'_{\mathbf{k}} & \sigma\Delta + \epsilon_{\mathbf{k}}^x \end{bmatrix} \\ \equiv \eta'_{\mathbf{k}} \mathbf{1} + \begin{bmatrix} -\sigma\Delta & \eta_{\mathbf{k}} \\ \eta_{\mathbf{k}} & \sigma\Delta \end{bmatrix} \quad (17)$$

where  $\eta'_{\mathbf{k}} \equiv \epsilon_{\mathbf{k}}^x = -2t \cos k_x$  and  $\eta_{\mathbf{k}} \equiv \epsilon_{\mathbf{k}}^y + \epsilon'_{\mathbf{k}}$ . Equation (17) is of the same form as Eq. (3), and therefore the quasiparticle energy eigenvalues and eigenvectors also retain their forms as in Eqs. (4) and (5).

Proceeding as earlier, we obtain for the transverse spin fluctuation propagator at the RPA level

where the magnon-mode energy is given by

$$\left(\frac{\omega_{\mathbf{q}}}{J}\right)^2 = \left\{ \left(1 + \frac{2J'}{J}\right) - (1 - \cos q_x) \right\}^2 - \left(1 + \frac{2J'}{J} \cos q_x\right)^2 \cos^2 q_y. \quad (19)$$

In the long wavelength limit, this reduces to

$$\left(\frac{\omega_{\mathbf{q}}}{2J}\right)^2 \approx \left(1 + \frac{2J'}{J}\right)^2 [\alpha q_x^2 + q_y^2], \quad (20)$$

where the coefficient of the  $q_x^2$  term,  $\alpha = \left(\frac{2J'}{J} - 1\right) / \left(1 + \frac{2J'}{J}\right)$ , becomes negative for  $2J' < J$ , indicating the instability of this F-AF phase. For  $2J' > J$ , Eq. (19) shows that there are no negative energy modes for any  $q_x, q_y$ , confirming the stability of this F-AF phase, in agreement with the finding that the relative sublattice magnetization orientation angle  $\theta = 0, \pi$ , [8] and not arbitrary as at the classical level.

$$[\chi^{-+}(\mathbf{q}, \omega)] = -\frac{1}{2} \left(\frac{3J}{\omega_{\mathbf{q}}}\right) \begin{bmatrix} 1 - \frac{2J'}{J}(1 - \gamma'_{\mathbf{q}}) - \frac{\omega}{3J} & -\gamma_{\mathbf{q}} \\ -\gamma_{\mathbf{q}} & 1 - \frac{2J'}{J}(1 - \gamma'_{\mathbf{q}}) + \frac{\omega}{3J} \end{bmatrix} \cdot \left(\frac{1}{\omega - \omega_{\mathbf{q}} + i\eta} - \frac{1}{\omega + \omega_{\mathbf{q}} - i\eta}\right), \quad (22)$$

where  $\gamma_{\mathbf{q}} = (\cos q_x + \cos q_y + \cos q_z)/3$  and  $\gamma'_{\mathbf{q}} = (\cos q_x \cos q_y + \cos q_y \cos q_z + \cos q_z \cos q_x)/3$ . The magnon-mode energy  $\omega_{\mathbf{q}}$  is given by

$$\omega_{\mathbf{q}} = 3J \left[ \left\{ 1 - \frac{2J'}{J}(1 - \gamma'_{\mathbf{q}}) \right\}^2 - \gamma_{\mathbf{q}}^2 \right]^{1/2}. \quad (23)$$

For small  $q$ , with  $\gamma'_{\mathbf{q}} \approx 1 - q^2/3$  and  $\gamma_{\mathbf{q}} \approx 1 - q^2/6$ , the magnon energy reduces to

$$\omega_{\mathbf{q}} = \sqrt{3}Jq \left(1 - \frac{4J'}{J}\right)^{1/2} \quad (24)$$

which vanishes in the limit  $J'/J \rightarrow 1/4$  due to the frustration effect of the NNN coupling  $J'$ . The softening of the low-energy magnon spectrum has a bearing on the Néel temperature,  $T_N$ , as discussed below.

Within the renormalized spin-fluctuation theory, [4]  $T_N$  is obtained from the isotropy condition  $\langle S^+ S^- + S^- S^+ \rangle_{T=T_N} = \frac{2}{3}S(S+1)$ . For  $J' = 0$ , the Néel temperature was obtained earlier as  $T_N = zJ \frac{S(S+1)}{3} f_{\text{SF}}^{-1}$  for the general case of spin  $S$  and  $z$  nearest neighbors on a hypercubic lattice. [4] For the simple cubic lattice the spin-fluctuation factor  $f_{\text{SF}} \equiv \sum_{\mathbf{q}} 1/(1 - \gamma_{\mathbf{q}}^2) = 1.517$ , and for  $S = 1/2$  this leads to  $T_N/J = 0.989$ . Extending this analysis to the present case, from Eq. (18) for the magnon propagator, we obtain

$$T_N = \frac{3J}{2} \left[ \sum_{\mathbf{q}} \frac{1 - \frac{2J'}{J}(1 - \gamma'_{\mathbf{q}})}{\left\{ 1 - \frac{2J'}{J}(1 - \gamma'_{\mathbf{q}}) \right\}^2 - \gamma_{\mathbf{q}}^2} \right]^{-1}. \quad (25)$$

The Néel temperature, evaluated from the above equation, is shown in Fig. 3 as a function of  $J'$ . The rapid

C.  $d = 3$

We now consider a simple cubic lattice and obtain the reduction in the Néel temperature due to the frustrating NNN spin coupling. In this case the lattice free-fermion energies are

$$\epsilon_{\mathbf{k}} = -2t(\cos k_x + \cos k_y + \cos k_z),$$

$$\epsilon'_{\mathbf{k}} = -4t'(\cos k_x \cos k_y + \cos k_y \cos k_z + \cos k_z \cos k_x), \quad (21)$$

and an extension of the earlier treatment for the two-dimensional case leads to

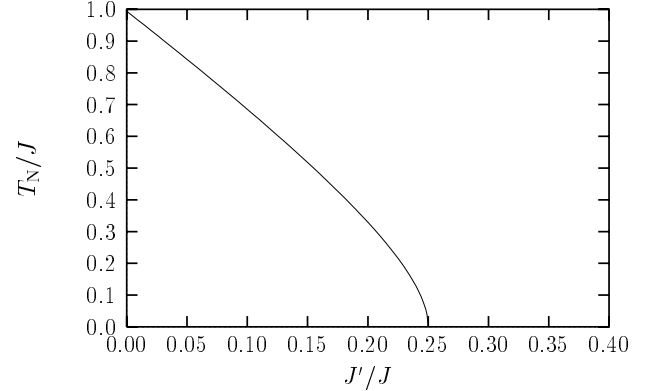


FIG. 3. The rapid decrease in the Néel temperature for the simple cubic lattice with the frustrating NNN spin coupling  $J'$ .  $T_N/J = 0.989$  for  $J'/J = 0$ .

reduction of  $T_N$  with  $J'$  and the vanishing at  $J' = J/4$  is due to the enhancement of transverse spin fluctuations arising from the frustration-induced softening of the long-wavelength, low-energy magnon modes. The instability at  $J' = J/4$  (or  $t' = t/2$ ) is towards a F-AF phase with ordering wavevector  $\mathbf{Q} = (0, \pi, \pi)$ , involving antiferromagnetic alignment of spins in planes and ferromagnetic alignment in the perpendicular direction.

### D. $\mathbf{Q} = (0, \pi, \pi)$ phase

In this section we study the transverse spin fluctuations in the F-AF broken-symmetry state with  $\mathbf{Q} = (0, \pi, \pi)$ , and examine the nature of the instability as  $J'$  approaches  $J/4$  from above. The instability can also be seen from energy considerations. The classical energy per spin for the two orderings are:  $E_{\text{AF}} = -6J + 12J'$  and  $E_{\text{F-AF}} = -2J - 4J'$ , so that the F-AF state becomes energetically favourable for  $J' > J/4$ . In three dimensions, the collinear  $\mathbf{Q} = (0, \pi, \pi)$  state is stable even at the classical level, unlike the degeneracy present in the  $d = 2$  case at this level.

In the  $\mathbf{Q} = (0, \pi, \pi)$  phase, the spins lying in the y-z plane (or any other parallel plane) are antiferromagnetically ordered, and hence the square lattice in this plane may be subdivided into two sublattices. Any site  $i$  with position coordinates  $(i_x, i_y, i_z)$  may then be uniquely placed in one of the two sublattices. The NN hopping terms in the y-z plane connect sites of opposite sublattices, while those in the x direction involve sites of the same sublattice. Therefore, the corresponding hopping energy terms  $\epsilon_{\mathbf{k}}^{yz} = -2t(\cos k_y + \cos k_z)$  and

$$\begin{aligned} [\chi^{-+}(\mathbf{q}, \omega)] = & -\frac{1}{2} \left( \frac{2J}{\omega_{\mathbf{q}}} \right) \times \\ & \left[ \left( 1 + \frac{2J'}{J} \right) - \frac{1}{2} \left\{ (1 - \cos q_x) + \frac{2J'}{J} (1 - \cos q_y \cos q_z) \right\} - \frac{\omega}{2J} \right. \\ & \left. - \left( 1 + \frac{2J'}{J} \cos q_x \right) \frac{1}{2} (\cos q_y + \cos q_z) \right. \\ & \left. \left( \frac{1}{\omega - \omega_{\mathbf{q}} + i\eta} - \frac{1}{\omega + \omega_{\mathbf{q}} - i\eta} \right) \right] \\ & - \left( 1 + \frac{2J'}{J} \cos q_x \right) \frac{1}{2} (\cos q_y + \cos q_z) \left[ \left( 1 + \frac{2J'}{J} \right) - \frac{1}{2} \left\{ (1 - \cos q_x) + \frac{2J'}{J} (1 - \cos q_y \cos q_z) \right\} + \frac{\omega}{2J} \right] \end{aligned} \quad (28)$$

where the magnon-mode energy is given by

$$\left( \frac{\omega_{\mathbf{q}}}{2J} \right)^2 = \left[ \left( 1 + \frac{2J'}{J} \right) - \frac{1}{2} \left\{ (1 - \cos q_x) + \frac{2J'}{J} (1 - \cos q_y \cos q_z) \right\} \right]^2 - \left( 1 + \frac{2J'}{J} \cos q_x \right)^2 \left( \frac{\cos q_y + \cos q_z}{2} \right)^2 \quad (29)$$

In the long wavelength limit, this reduces to

$$\left( \frac{\omega_{\mathbf{q}}}{2J} \right)^2 \approx \frac{1}{2} \left( 1 + \frac{2J'}{J} \right) [\alpha q_x^2 + q_y^2 + q_z^2], \quad (30)$$

where the coefficient of the  $q_x^2$  term,  $\alpha = \left( \frac{4J'}{J} - 1 \right)$ , decreases as  $J'/J$  approaches 1/4 from above, vanishes at  $J'/J = 1/4$ , and eventually becomes negative for  $J'/J < 1/4$ . This signals the instability of the F-AF phase at  $J'/J = 1/4$ , and the above provides a description of the transition from the F-AF side of the phase boundary.

The spin-fluctuation correction  $\delta m_{\text{SF}}$  in the F-AF phase, evaluated from Eqs. (16,28,29) in analogy with the  $d = 2$  result in Eq. (15), is shown in Fig. 4. The correction in the AF phase is also shown for comparison. Near the transition point  $J'/J = 1/4$ , the correction in the F-AF phase is seen to be nearly half of that in the AF phase, indicating greater robustness of the F-AF phase

$\epsilon_{\mathbf{k}}^x = -2t \cos k_x$  will occupy, in the two-sublattice basis, off-diagonal and diagonal positions, respectively. Similarly for NNN hopping  $\epsilon_{\mathbf{k}}'^{yz}$  is diagonal, whereas  $\epsilon_{\mathbf{k}}'^{xy}$  and  $\epsilon_{\mathbf{k}}'^{zx}$  are off-diagonal. Thus the HF Hamiltonian matrix takes the form

$$\begin{aligned} H_{\text{HF}}^{\sigma}(\mathbf{k}) = & \begin{bmatrix} -\sigma\Delta + \epsilon_{\mathbf{k}}^x + \epsilon_{\mathbf{k}}'^{yz} & \epsilon_{\mathbf{k}}^{yz} + \epsilon_{\mathbf{k}}'^{zx} + \epsilon_{\mathbf{k}}'^{xy} \\ \epsilon_{\mathbf{k}}^{yz} + \epsilon_{\mathbf{k}}'^{zx} + \epsilon_{\mathbf{k}}'^{xy} & \sigma\Delta + \epsilon_{\mathbf{k}}^x + \epsilon_{\mathbf{k}}'^{yz} \end{bmatrix} \\ \equiv & \eta'_{\mathbf{k}} \mathbf{1} + \begin{bmatrix} -\sigma\Delta & \eta_{\mathbf{k}} \\ \eta_{\mathbf{k}} & \sigma\Delta \end{bmatrix} \end{aligned} \quad (26)$$

where

$$\begin{aligned} \eta'_{\mathbf{k}} \equiv & \epsilon_{\mathbf{k}}^x + \epsilon_{\mathbf{k}}'^{yz} = -2t \cos k_x - 4t' \cos k_y \cos k_z \quad (27) \\ \eta_{\mathbf{k}} \equiv & \epsilon_{\mathbf{k}}^{yz} + \epsilon_{\mathbf{k}}'^{zx} + \epsilon_{\mathbf{k}}'^{xy} = [-2t - 4t' \cos k_x](\cos k_y + \cos k_z) \end{aligned}$$

Eq. (26) is of the same form as Eq. (3), and therefore the quasiparticle energy eigenvalues and eigenvectors also retain their forms as in Eqs. (4) and (5).

Proceeding as earlier, we obtain for the transverse spin fluctuation propagator at the RPA level

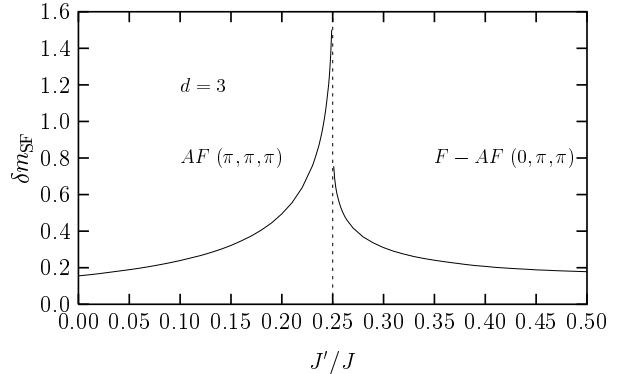


FIG. 4. The spin-fluctuation correction to sublattice magnetization in the AF and the F-AF phases.

with respect to quantum spin fluctuations. The spin-fluctuation correction in both phases approaches 1 (the HF value of sublattice magnetization) only very close to

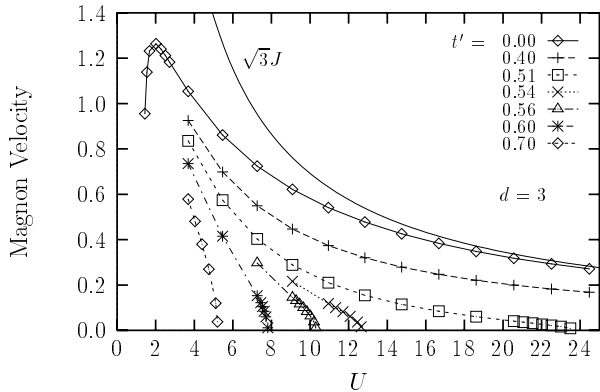


FIG. 5. The magnon velocity vs.  $U$  for several values of the NNN hopping  $t'$ . For  $t' > 1/2$  the magnon velocity vanishes at finite  $U_c$ , above which the AF phase is unstable to transverse perturbations.

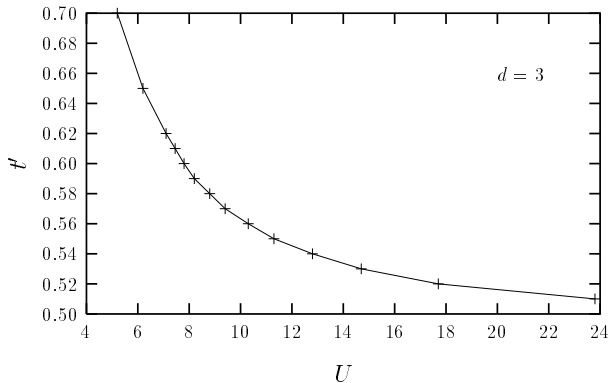


FIG. 6. The  $U$ -dependence of the critical  $t'$  values at which the magnon velocity vanishes. The critical  $t'$  value approaches  $1/2$  as  $U \rightarrow \infty$ .

the critical value  $J'/J = 1/4$ . This implies that (up to first order)  $m$  vanishes only very close to  $J'/J = 1/4$ , so that the extent of the spin-disordered phase is quite narrow. This is unlike the  $d = 2$  case, where the AF order is lost at  $J'/J \approx .37$ , well before the F-AF state appears at  $J'/J \gtrsim 0.5$ .

## V. MAGNETIC PHASE DIAGRAM

In section IV we analytically studied the transverse spin fluctuations in the strong coupling limit, and showed from an RPA analysis how the frustration induced due to the magnetic competition between the NN and NNN AF spin couplings  $J$  and  $J'$  leads to an instability of the AF phase towards a F-AF phase at  $t'/t = 1/\sqrt{2}$  for the square lattice and  $t'/t = 1/2$  for the simple cubic lattice. In this section we extend this study and obtain the AF—F-AF phase boundary in the full  $U$ -range. As the

instability is signalled by the vanishing of the magnon velocity,

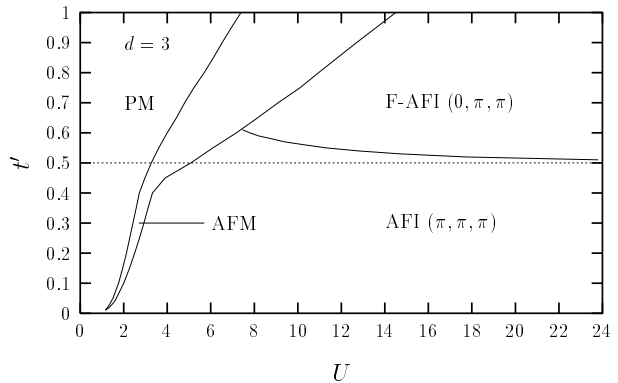


FIG. 7. The magnetic phase diagram of the  $t-t'$ -Hubbard model in the finite band gap region. The small deviation in the phase boundary from  $t' = 1/2$  is due to the stabilization of the AF phase by the NNN ferromagnetic coupling generated at finite  $U$ .

we numerically evaluate the magnon velocity in the AF state for several  $U$  values, except for the weak coupling side where the band gap vanishes. For this purpose, the matrix  $[\chi^0(\mathbf{q}, \omega)]$  is evaluated for a fixed small  $q$  by numerically performing the  $\mathbf{k}$ -summation in Eq. (8). From the eigenvalues  $\lambda_{\mathbf{q}}(\omega)$  obtained at several  $\omega$  values, the magnon-mode energy is then obtained from  $1 - U\lambda_{\mathbf{q}}(\omega_{\mathbf{q}}) = 0$  using interpolation. The ratio  $\omega_{\mathbf{q}}/q$  yields the magnon velocity.

The  $U$ -dependence of the magnon velocity is shown in Fig. 5 for several  $t'$  values in the range  $0 \leq t' \leq 0.7$ . For  $t' > 0.5$ , the magnon velocity vanishes at a finite critical interaction strength  $U_c$ , above which the AF state is unstable towards the F-AF phase. In the limit of vanishing magnon velocity the Néel temperature tends to zero, as the thermal excitation of magnons at any finite temperature leads to a divergence in the transverse spin fluctuations. Hence the AF—F-AF transition is a quantum phase transition. The critical  $t' - U$  curve, which forms the phase boundary of the AF—F-AF transition, is shown in Fig. 6. The low- $U$  region ( $U \lesssim 7$ ) of this boundary is not relevant as the band gap actually vanishes, and the intraband processes will also have to be included. This yields the magnetic phase diagram of the  $t - t'$ -Hubbard model in the insulating region, as shown in Fig. 7. It is clear that the NNN ferromagnetic coupling generated for finite  $U$  provides a delicate correction to the AF—F-AF transition which occurs at  $t'/t = 1/2$  in the  $U/t \rightarrow \infty$  limit.

## VI. CONCLUSIONS

The RPA-level magnon propagator is analytically evaluated in the strong coupling limit, both in the AF

$(\pi, \pi, \pi)$  and the F-AF  $(0, \pi, \pi)$  states. As expected, the frustration-inducing NNN hopping  $t'$  sharply enhances the quantum spin-fluctuation correction to sublattice magnetization, reducing the zero-temperature AF order in two dimensions. This enhancement arises from a softening of the magnon modes, which is clearly seen in the magnon density of states as a pronounced transfer of spectral weight to lower energy region. This frustration-induced magnon softening also enhances the thermal excitation of magnons at finite temperature, causing a sharp drop in the Néel temperature in three dimensions.

With increasing  $t'$  and frustration, the magnon velocity eventually vanishes as  $t'/t \rightarrow 1/\sqrt{2}$  in  $d = 2$  and  $t'/t \rightarrow 1/2$  in  $d = 3$  (both for  $U/t \rightarrow \infty$ ). This vanishing of the magnon velocity is symptomatic of an instability of the AF state, which is towards the  $(0, \pi)$  state in  $d = 2$  and the  $(0, \pi, \pi)$  state in  $d = 3$ , both involving ferromagnetic ordering in one direction. A numerical evaluation of the magnon velocity in  $d = 3$  as a function of  $U$  allows this phase boundary to be tracked in the full range of interaction strength, indicating that the AF state  $(\pi, \pi, \pi)$  is interestingly stabilized with decreasing  $U$ . The reduction in the degree of frustration due to the extended-range spin couplings generated for finite  $U$  provides a simple physical understanding of this result.

While in this paper we have confined our attention to the finite-gap insulating region (AFI) of the phase diagram, a prominent gapless metallic region also exists in  $d = 3$ , which brings in a fundamentally new ingredient. In the insulating state, the basic particle-hole propagator  $\chi^0(\mathbf{q}, \omega)$  involves only interband processes, and it is the competition between the  $t$  and  $t'$  terms which can lead to a vanishing magnon velocity and an instability. This competition is much more complex in the metallic AFM state, where intraband particle-hole processes are also present. A full stability analysis of this antiferromag-

netic metallic (AFM) state will be discussed separately. [19]

- 
- <sup>1</sup> J. R. Schrieffer, X.-G. Wen, and S.-C. Zhang, Phys. Rev. B **39**, 11663 (1989); **41**, 4784(E) (1990).
  - <sup>2</sup> A. Singh and Z. Tešanovič, Phys. Rev. B **41**, 614 (1990); Phys. Rev. B **41**, 11 457 (1990).
  - <sup>3</sup> A. Singh, Euro. Phys. Jour. B **11**, 5 (1999).
  - <sup>4</sup> A. Singh, Report No. cond-mat/9802047.
  - <sup>5</sup> A. Singh, Report No. cond-mat/0006079.
  - <sup>6</sup> A. Singh, Phys. Rev. B **43**, 3617 (1991).
  - <sup>7</sup> P. Chandra and B. Doucot, Phys. Rev. B **38**, 9335 (1988).
  - <sup>8</sup> A. Moreo, E. Dagotto, Th. Jolicoeur, and J. Riera, Phys. Rev. B **42**, 6283 (1990).
  - <sup>9</sup> A. Singh, Phys. Rev. B **48**, 6668 (1993).
  - <sup>10</sup> P. Bénard, L. Chen, and A. -M. S. Tremblay, Phys. Rev. B **47**, 589 (1993); A. Veilleux, A. Daré, L. Chen, Y. M. Vilck, and A. -M. S. Tremblay, Phys. Rev. B **52**, 16255 (1995).
  - <sup>11</sup> T. Tohyama and S. Maekawa, Phys. Rev. B **49**, 3596 (1993).
  - <sup>12</sup> G. Stemmman, C. Pépin, and M. Lavagna, Phys. Rev. B **50**, 4075 (1994).
  - <sup>13</sup> O. K. Andersen, A. I. Liechtenstein, O. Jepsen, and F. Paulsen, J. Phys. Chem. Solids **56**, 1573 (1995).
  - <sup>14</sup> A. V. Chubukov and K. A. Musaelian, J. phys., Condens. Matter, **7**, 133, (1995).
  - <sup>15</sup> D. Duffy and A. Moreo, Phys. Rev. B **52**, 15607 (1995).
  - <sup>16</sup> D. Duffy and A. Moreo, Phys. Rev. B **55**, 676 (1997).
  - <sup>17</sup> W. Hofstetter and D. Vollhardt, Ann. Phys. (Leipzig) **7**, 48 (1998).
  - <sup>18</sup> P. Sen and A. Singh, Phys. Rev. B **48**, 15792 (1993).
  - <sup>19</sup> A. Singh, (to be published).